CROSS FLOW EFFECTS ON THE FLAME HEIGHT OF AN INTERMEDIATE SCALE DIFFUSION FLAME

Gilles Kolb, Jose L. Torero

Department of Fire Protection Engineering
University of Maryland
College Park, MD20742, USA

Jean-Michel Most and Pierre Joulain

Laboratoire de Combustion et de Détonique
UPR9028 au CNRS-ENSMA-Université de Poitiers
86960 Futuroscope CEDEX, France

ABSTRACT

An experimental study has been conducted at an intermediate scale to study the effect of a cross flow on a purely buoyant fire. Video taping of the flame and post processing of the images by means of a novel technique provide a contour of a mean flame for all cases studied. This flame contour allows the determination of a mean flame length and a mean flame height. The mean flame length and height are recorded as functions of the forced flow velocity. Three dimensional flow patterns are formed in the flame trailing edge affecting both the mean flame length and height. The three dimensional patterns are studied systematically as functions of the cross flow velocity to quantify the effect of confinement on the flame geometry.

INTRODUCTION

Most fires grow in the presence of some kind of cross flow, urban fires and forest fires spread in the presence of wind and most buildings fires are tilted by cross flows which can come from ventilation or flow constrictions. One of the most classical configuration is a pool fire tilted by a cross wind. During the initial stages of the spread process the flame is confined within a boundary layer and as the size of the burning surface increases the flame stands up because of the dominance of upward buoyancy over the horizontal wind force. If the geometrical boundaries lie within the zone influenced by the flame, particular flow patterns tend to affect the flame geometry. A common example will be that of a fire inside a tunnel. If the characteristic length scale of the flame is of the same order of that of the tunnel, the flow will interact with the walls creating re-circulation zones. Tunnels generally have ventilation systems, therefore, the combined influence of the geometrical constraints and the forced flow needs to be studied.

The study of flames inside boundary layer flows can be traced to the pioneering study of a reacting laminar boundary developed by Emmons [1]. This work showed that the evaporation rate of fuel could be expressed as a function of the mass transfer number only. A good review of the work that followed this study was done by Williams [2] who described experimental studies conducted with solid and liquids fuels. Studies that focused on the aerodynamic structure of the flame have used a porous bed burner to de-couple heat and fuel transport mechanisms. This approach permits fuel and oxidizer to be varied independently and unlimited experimentation time. Examples of the use of this technique in a similar configuration to this study are those of Hirano et al. [3] and Ramachandra et al. [4].

The hazard level of a specific fire scenario is intimately related to the flame geometry. The knowledge of the size of the flame, as a function of the size of the pyrolyzing fuel, will determine how the flame will interact with its

surroundings. In general, the geometry of the flame is conditioned by the characteristics of the environment and although fire scenarios can be classified in specific groups, considerations need to be made for different flow conditions and geometrical constraints.

Several studies have concentrated on the flame shape of a fire tilted by a cross flow in the past [5, 6, 7, 8, 9, 10, 11, 12, 13]. Thomas [5] studied wood crib fires subject to a cross flow and measured the flame length as a function of the flow velocity for a specific fuel size. It was observed that the flame length decreased with the cross flow velocity. Thomas concluded that at higher flow velocities mixing is enhanced resulting in a decrease in the flame length. Rios [8] conducted a series of experiments with the same type of fuel and, contrary to the observations of Thomas [5], his results showed an independence between the flame length and the forced flow velocity. Based on these observations Rios [8] correlated his data and obtained similar expressions to those previously obtained by Anderson et al. [7] and Rothermel [11] when they studied the flame spread process on mat type fuel beds. The different expressions obtained by these two authors for the flame height only differ in the power law used to describe the fuel, this discrepancy can be attributed to the different fuel type. Simmilar experiments were conducted by Putnam [9] who study the fuel size effect by using circular fuel sources of different diameters. Putnam [9] describes the flame geometry by means of two parameters, the flame extension and the flame height. The effect of a cross flow on these two geometrical characteristics is then studied for a point source, area source and line source. General expressions for the flame extension and height are extracted from data correlation and result in power law functions of a Froude number based on the mean flame height without cross wind. Larger scale flames have been studied on water [14] or in a large scale wind tunnel while focusing on the fire spread process [11, 12,13]. Apte et al [12] divided the flame in two characteristic modes, a boundary layer mode and a plume mode. The boundary layer mode, occurring near the fuel leading edge, is almost linear and is replaced by a plume like flame (plume mode) as the distance from the leading edge increases.

Following the work of Putnam [9], the present work studies the effect of a cross flow on the flame length and height for the specific configuration of an intermediate scale flame confined in a tunnel of similar characteristic length scale as that of the fire. This work relies on a parametric study of a simulated pool fire done on the same experimental facility without a cross-flow [15, 16]. The geometrical characteristics of the flame have been determined for different cross flow velocities, fuel injection surface and velocity.

EXPERIMENTAL APPARATUS

A schematic diagram of the wind tunnel is presented in figure 1. The experimental apparatus consists of a 5.25 m long horizontal channel through which air motion was induced by means of a centrifuge fan. The center part of the wind tunnel is the test section, 1.75m long, 0.7 m height and 0.4 m wide (2 on figure 1). The walls, floor and ceiling are each made of seven removable actively cooled panels (0.7 m x 0.4 m for the walls and 0.4 m x 0.25 m for floor and ceiling). The wall panels can be substituted by windows, for observation, and the floor panels by burners. The burner covers the entire cross section of the tunnel.

Each burner consists of a rectangular sintered bronze slab (20 mm in thickness) with imbedded copper cooling tube (8 mm in diameter). The thickness of the slab and the diameter are chosen to guarantee homogeneous flow through the entire burner surface. Three burners surfaces are used during this work, all burners are 0.4 m in width and vary in length, 0.25 m, 0.5 m, and 0.75 m. Being the length the stream wise direction. Water form a reservoir at constant temperature of 65°C was pumped through the cooper tube to keep the burner surface at a given temperature and to avoid condensation [17]. Similar burner have been used successfully in the past to simulate the pool fire combustion of a liquid or a solid fuel [18, 19, 20].

Experiments were conducted with commercial propane. The fuel flow is regulated by a mass flow meter (BROOKS 5812N). Commercial propane is a mixture of hydrocarbons and its principal constituents in mass are Propylene (51%), Propane (33%), Isobutane (12%), and n-butane (2.3%) with 1.7 % of other hydrocarbons.

The focus of this work is on flame characteristics of fires. Fire flames are in general buoyancy dominated and therefore characterized by a low initial mass transport. Two parameters are commonly used to characterize fire flames:

- The source Froude number which is defined as the ratio between buoyant and inertia forces :

$$Fr = \frac{V_f^2}{gD} \tag{1}$$

- The dimensionless heat release rate as defined by Zukoski [21]:

$$Q_D^* = \frac{Q}{\rho_\infty C_p T_\infty \sqrt{gD}\, D^2} \tag{2}$$

Flames characteristic of fires have source Froude number of the order of 10^{-4} - 10^{-6} [22], and Q_D* below the unity [21]. For all experimental conditions, these two fundamental parameters describing the flame are chosen to be similar to those corresponding to fire scales flames.

The characteristic velocity of the main flow is given by a screw gauge placed in the symmetry plane of the test section at a height of 0.55 m from the floor and 0.5 m upstream of the burner leading edge. The rotating frequency of the fan is regulated to keep the flow velocity measured by the gauge constant through out an experiment. The velocity measured by the gauge was used as the reference in this work.

The air is conducted into the test section through a convergent (1 on figure 1), 1.8 m long, with a restriction ratio of 3.57. To homogenize the flow, a honeycomb, 50 mm in thickness, is fixed at the entry of the convergent. Combustion products are collected in a collector (3 on figure 1) 1.7 m long. To minimize environmental perturbations present in the laboratory, the floor of the channel is placed 900 mm from the room floor. An initial aerodynamic study of the wind tunnel pointed out that the best method to induce a fully developed velocity profile upstream from the burner is by means of aspiration. Aspiration and blowing experiments were also conducted with flames and showed no significant differences. The geometry was chosen to guarantee, keeping minimum dimensions, that the flow will reproduce a turbulence intensity ($u'/\overline{U}$) typical of fire scenarios ($5\% < u'/\overline{U} < 15\%$ [23]). The measured turbulence intensity inside the test section is, for all conditions studied, was of the order of $u'/\overline{U} \approx 7\text{-}10\%$ and originates in the convergent of the wind tunnel [24].

A CCD camera (Sony DXC-300A) was used tom record the visual characteristic of the flame on a U-matic video recorder (Sony BVU-150 P). The image processing used to extract the length and height of the flame is an extension of a technique described elsewhere [16, 19)], therefore will not be presented here. Temperature measurements were conducted with 50μm type K thermocouples.

Three parameters are varied during this study, the cross flow velocity, the combustible injection velocity and the burner length. The range of values for the air flow velocity (U_∞) is imposed by the experimental apparatus and allows to change the air velocity from 0.5 m/s to 2.5 m/s. The fuel injection velocity (V_f) is restricted by the source Froude number which is kept in the range from 10^{-6} to 10^{-4}. The values used for the fuel injection velocity are: 1.945 mm/s, 2.919 mm/s, 3.891 mm/s and 4.864 mm/s. All three burner sizes were used: 0.25 m, 0.50 m and 0.75 m. As the fuel velocity is kept constant when changing the burner length, the theoretical heat release rate, Q, varied in the range 18 kW to 135 kW.

EXPERIMENTAL RESULTS AND DISCUSSION

Pool fires are not stationary flames instead they fluctuate with a characteristic frequency. This phenomena and the fluctuation frequency have been extensively described in the literature [21] and generally and average flame shape and height needs to be extracted to characterize pool fires. Zukoski et al [21,25] defined the mean flame height of a pool fire as the elevation where flame intermittence is 50%. For this particular configuration, the fluctuations, typical of pool fires, are still present in the main flow direction, but with no detachment of flame pockets, therefore, the same criterion is used to define the mean flame extension. An image by image analysis allows to extract the fluctuation frequency but this aspect of the problem goes beyond the scope of this work.

The mean flame is defined as where the intermittence is 50% (figure 2(a)). The zone where the intermittence is 50% is finite, therefore, to obtain the mean flame border the arithmetic average of the internal and external boundaries of the 50% intermittence zone is taken and defined as the mean flame border (figure 2(b)). The flame extension (X_f) is defined as the maximum horizontal distance from the leading edge of the burner to the average flame border (X_f in figure 2(c)) and the flame height (Y_f) is the maximum vertical distance from the mean flame border to the floor of the test section. The mean flame border, the flame extension and the flame height will be used to try to describe the effect of a cross flow in a confined buoyant flame.

For $U_\infty < 1$ m/s the flame is buoyantly dominated and only perturbed by the forced flow. Close to the burner leading edge the flame border is almost linear, rapidly replaced by a flame like plume. This regime is similar to the plume mode described by Apte et al. (1991a). For $U_\infty \geq 1$ m/s inertia becomes dominant and buoyancy limits its influence to the flow around the flame. The flame is linear for the entire range of velocities studied. The flame is now in a mode described as the boundary layer mode by Apte et al [12]. Figure 3(a) shows a typical case of a flame mostly in the buoyant plume mode and figure 3(b) a flame in the boundary layer mode.

As mentioned before, the burner covers the entire cross section of the wind tunnel. This geometric characteristic results in a three-dimensional flow pattern that could be observed by means of a top view of the flame. In order to obtain a top view of the flame two ceilings panels are replaced by a window. The mean presence probability of a flame tilted by 1.5 m/s forced flow is presented on figure 4. A lateral flame contraction is observed beyond the burner ($x>X_b$), for all configurations studied. The flame width corresponds to that of the burner (Z_b) for $x<X_b$, as the flame exits the burner zone it becomes thinner (Z'). The flame contraction requires significant attention since it is a product of the geometrical constraints imposed by the test section and it affects the flame length and height.

As noted by Apte et al [12], the rate of oxidant entrainment over the flame height is in stoichiometric (r) proportion to the rate of fuel pyrolysis:

$$\frac{\int_0^{Y_F} Z' \rho_\infty U(y) dy}{\int_0^{X_b} Z \rho_f V_f dx} = r \tag{3}$$

furthermore, Torero et al. [26] showed that a linear flame border corresponded to a flame where mass transport was dominated by convection and where the flame height could be derived by means of the following expression:

$$Y_F = C \frac{V_f}{U_\infty} X_F \tag{4}$$

where C is a constant. These expressions clearly show that the contraction affects both the flame length (X_F) and height (Y_F).

The ratio (Z_b/Z') was studied systematically as a function of the oxidizer flow velocity. It was observed that the contraction became more pronounced as the forced flow velocity increases resulting in an increasing value of Z_b/Z'. Figure 5 shows characteristic variations of the Z_b/Z' ratio for constant burner length (figure 5(a)) and injection velocity (figure 5(b)). The Z_b/Z' ratio increases linearly with the forced flow velocity, with a constant slope as the fuel injection velocity increases and an increasing slope as the burner length decreases. Both fuel injection velocity and burner length contribute to neutralize the three dimensional effects that lead to the contraction of the flame downstream of the burner. The change in slope when increasing the size of the burner points towards a coupled effect of buoyancy and characteristic length scale. The results shown in figures 5(a) and (b) are representative of all other experiments conducted.

Figures 6 and 7 show the dependency of the flame length and height on the oxidizer flow velocity for different heat release rates. An increase in the heat release rate results in an increase in both flame length and height for all oxidizer flow velocities studied. Figure 6 also shows a linear increase in flame length with U_∞. For Q=18 kW, X_f increases linearly with U_∞ only for U_∞ <1m/s but as the oxidizer velocity increases beyond 1 m/s the flame length

attains an almost constant value. This discrepancy between the 18 kW flame and all the others might be attributable to the limitations of the technique used to extract the average flame length. The flame in this case is very small and close to the burner resulting in a decreased luminous intensity that can lead to errors in the estimation of the average flame border. Contrary to the above observation, the flame height increases with U_∞ for U_∞<1 m/s and decreases for U_∞> 1m/s. It was previously reported by Kolb et al. [16] that in this same configuration the flame transitions from the buoyancy dominated regime to the forced flow regime at U_∞=1 m/s. In the buoyancy dominated regime, the incoming air is entrained towards the axis of symmetry of the test section by buoyancy. Natural convection in the direction perpendicular to the flow plane (z-direction) is of great significance. As U_∞ increases oxidizer transport in the z-direction decreases (the flame is tilted downstream) and the buoyancy dominated zone is displaced downstream of the burner. The result is an increase in the flame height. In the boundary layer mode, transport of oxidizer is dominated by the forced flow, therefore the flame height decreases with U_∞. It is important to note that although the transition from a plume to a boundary layer mode can not be seen when looking at the flame length or the contraction, it is consistent with the observation that the ratio Z_b/Z' increases with U_∞ and does not conflict with a linear increase X_F with U_∞. As shown by Kolb et al. [16], simple observation of an average visible flame might be misleading of the flow structure, temperature and velocity measurements generally give a better indication of the nature of the flow.

CONCLUSIONS

An experimental study was conducted to determine the geometrical characteristics of a flame representative of a fire subject to a cross-flow and confined by a duct of comparable dimensions to the flame. The parameters used to describe the geometrical characteristics of the flame were the flame length (X_F), flame height (Y_F) and the contraction ratio (Z_b/Z').

It was observed, at least for the present configuration, that the flame transitions from a plume mode to a boundary layer mode for U_∞>1m/s. The transition is only evident in the flame height and when observing the shape of the mean flame border.

It can also be concluded that:

- X_F increases linearly with U_∞
- Y_F increases with U_∞ when the flame is in the plume mode.
- Y_F decreases with U_∞ when the flame is in the boundary layer mode.
- Z_b/Z' increases linearly with U_∞ and decreases with both the fuel injection velocity and the burner size. Although the fuel injection velocity and burner size are inversely proportional to Z_b/Z' the dependency on V_f and X_b is not the same, therefore, can not be summarized to a dependency on Q as it is commonly done for pool fires.

REFERENCES

1. Emmons, H., Z. Agnew. Math. Mech., 36, 60-71, 1956

2. Williams, F.A., Combustion theory, 2nd Edition, The Benjamin Cummings Publishing Company Inc., Menlo Park, CA, 485-519, 1985

3. Hirano, T. and Kanno, Y, Fourteenth Symposium (International) on Combustion, The Combustion Institute, 391-398, 1973

4. Ramachandra, A. & Raghunandan, B. N, Combustion Science and Technology, 36, 109-121, 1984

5. Thomas, P., Ninth Symposium (International) on Combustion, The Combustion Institute, 844-859, 1963

6. Thomas, P., F.R. Note N°600, Fire Research Station, 1965

7. Anderson, H., E., and Rothermel, R., C, Tenth Symposium (International) on Combustion, The Combustion Institute, 1009-1019, 1965

8. Rios, J., Interaction effects of wind-blown proximate flames from burning wood cribs, PhD. Thesis, The University of Oklahoma, 1966

9. Putnam, A., A., Tenth Symposium (International) on Combustion, The Combustion Institute, 1039-1046, 1965

10. Pipkin, O.A. & Sliepcevich, C.M., I&EC Fundamentals, 3, N° 2, 147-154, 1964

11. Rothermel, R.C., Proceedings of the International Conference on Forest Fire Research, Coimbra, Portugal, 1-19, 1990

12. Apte, V.B., Bilger, R.W., Green, A.R. & Quintiere, J. G., Combustion and Flame, 85, 169-184, 1991

13. Apte, V.P., Green, A.R & Kent, J.H., Fire Safety Science-Proceedings of the Third International Symposium, 425-434, 1991

14. Raj, P. P. K. , Moussa, A. N. & Aravamudan, K, U.S. Coast Guard Report No. CG-D-55-79, 1979

15. Kolb, G., Etude d'une flamme non prémelangée caractéristique d'un incendie en présence d'un écoulement forcé, Ph.D. Thesis, Université de Poitiers, France, 1996

16. Kolb, G., Most, J. M. & Torero, J. L., ASME National Heat transfer Conference, Baltimore, 3, 19-35, August 1997

17. De Ris, J. & Orloff, L, Fifteenth Symposium (International) on Combustion, The Combustion Institute, 175-182, 1975

18. Audouin, L., Etude de la Structure d'une Flamme Simulant un Incendie de Produits Industriels. Caractérisation et Modélisationde Réels de Feux, Ph.D. Thesis, Université de Poitiers, France, 1995

19. Audouin, L., Kolb, G., Torero, J. L. and Most J. M., Fire Safety Journal, 24, 167-187, 1995

20. Most, J. M., Sztal, B. & Delichatsios M. A., Second International Symposium on Application of Laser Anemometry to Fluid Mechanics, Lisbon, Portugal, 1984

21. Zukoski, E.E., Kubota, T. & Cetgen, B.M., Fire Safety Journal, 3, 107-121, 1980/81

22. McCaffrey, B. J., NBSIR 79-1910, National Bureau of Standards, Washington D.C., 1979

23. Zhou, L. & Fernandez-Pello, A.C, Combustion and Flame, 92, 45-59, 1993

24. Rebuffet, P., Aérodynamique Expérimentale", Tome 2, Ed. Dunod, 1966

25. Zukoski, E. E., Cetegen,B. M. & Kubota, T., 20th Symposium (International) on combustion, the combustion Institute, 361-366, 1984

26. Torero, J.L., Bonneau, L., Most, J. M. & Joulain, P, Twenty-Fifth Symposium (International) on Combustion, The Combustion Institute, 1701-1709, 1994

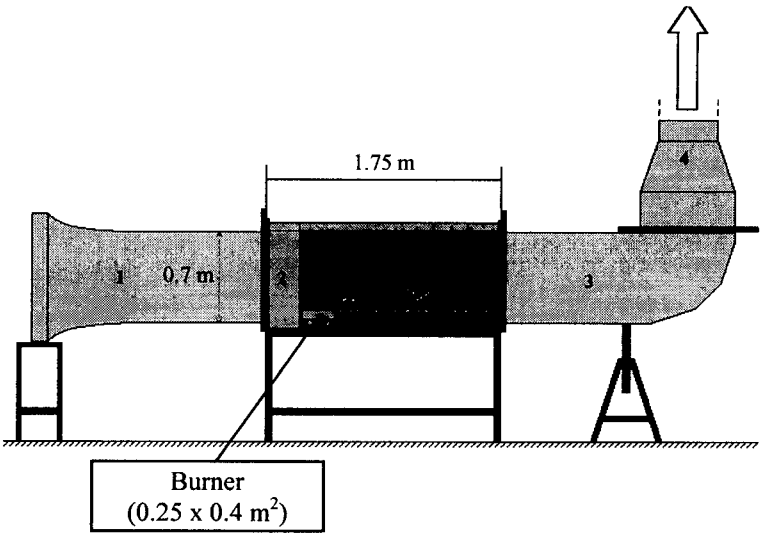

Fig.1 Experimental apparatus in a real situation.

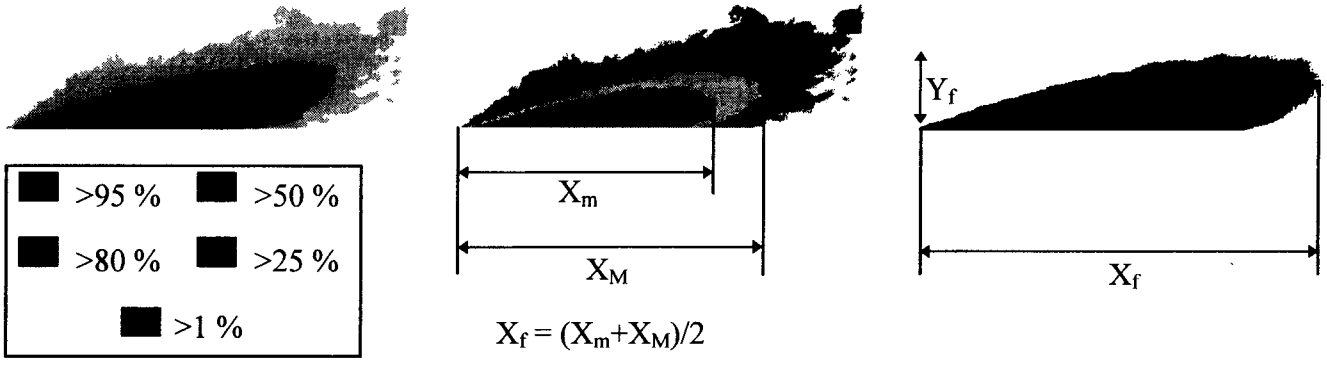

Fig. 2 Example of images processing from which the mean distance are extracted.

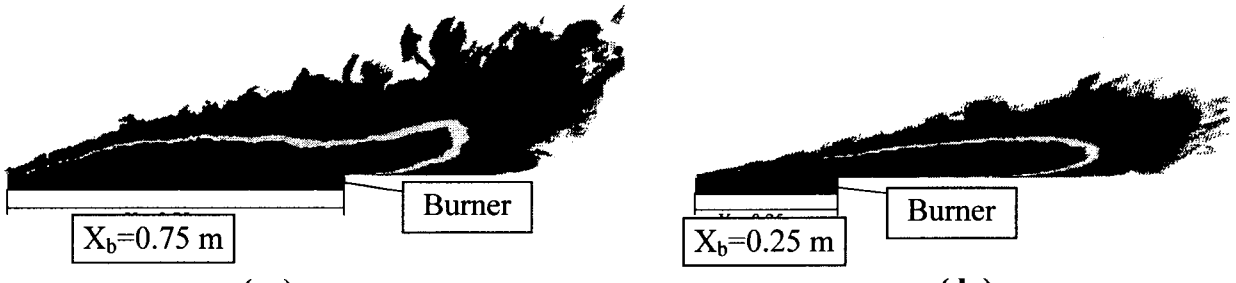

Fig. 3 Presence probability of the flame in the plume mode (a) and boundary layer mode (b).

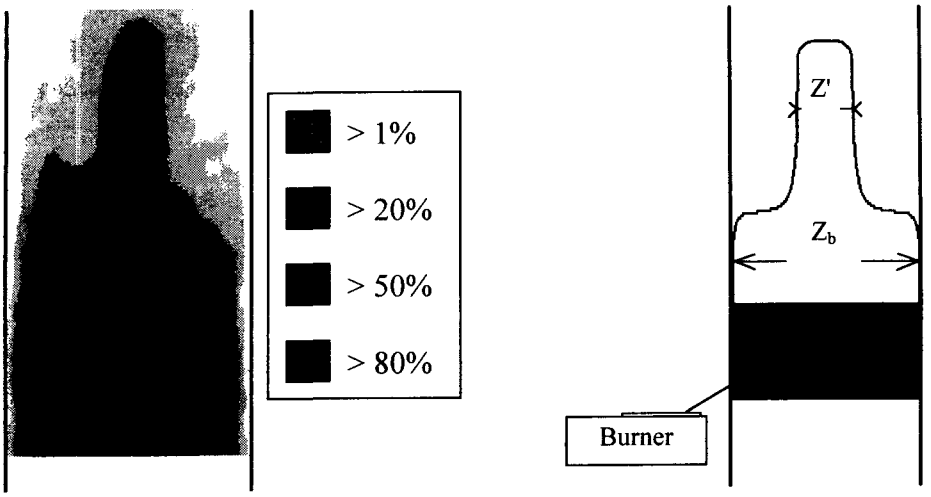

Fig. 4 Presence probability of the flame in the transversal plane.

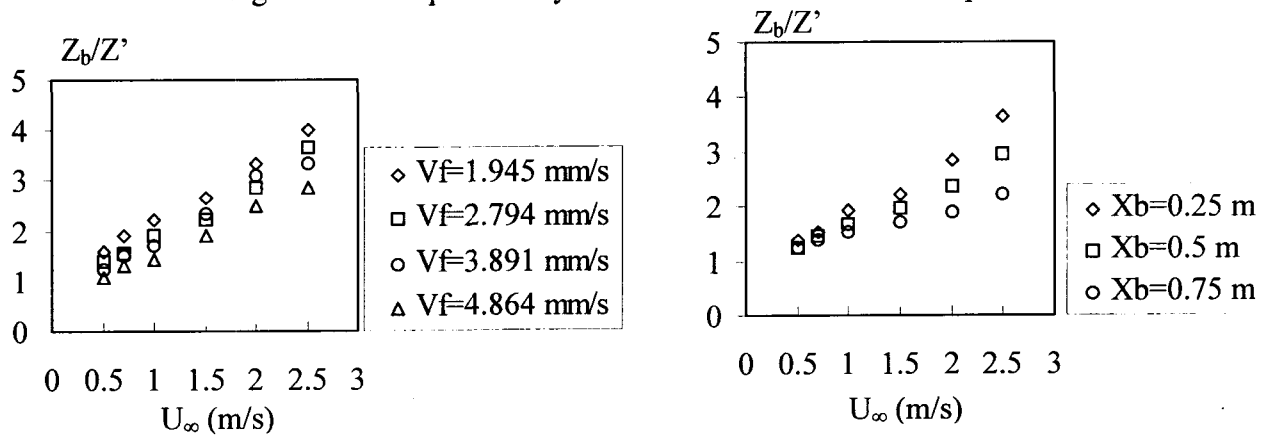

(a) (b)

Fig. 5 Evolution of the ratio Z_b/Z' for a constant burner length X_b=0.25m (a) and a constant fuel injection velocity V_f=2.974 mm/s (b).

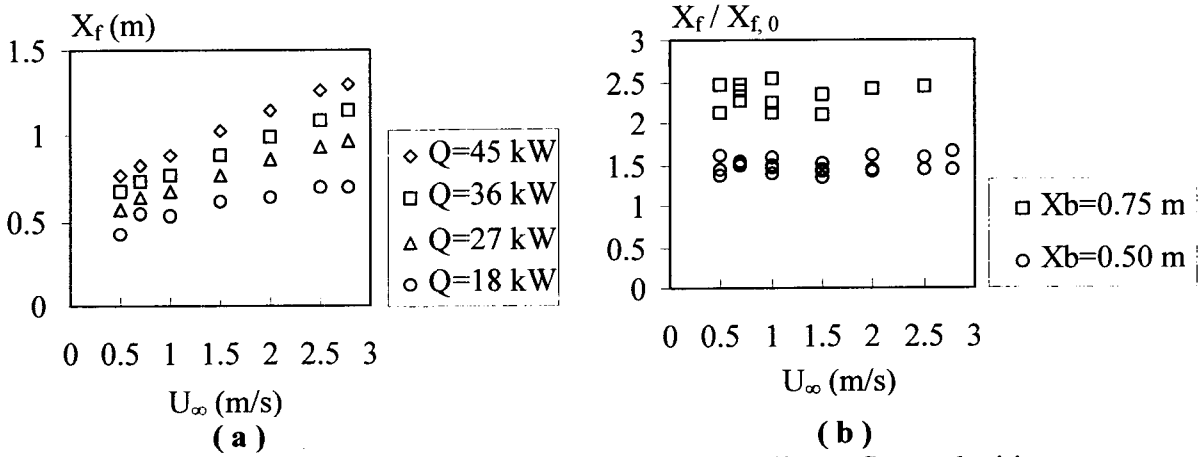

(a) (b)

Fig. 6 Evolution of the mean flame length for different flow velocities

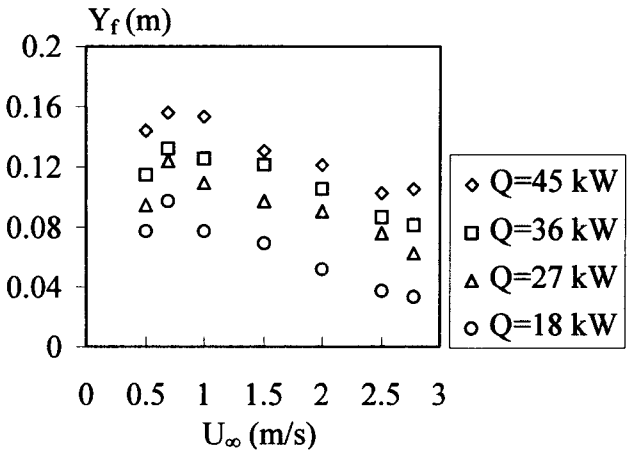

Fig. 7 Evolution of the mean flame height for different flow velocities